

Monitoring of Rapid Land-cover Change in the Intensified Grazing Area of North Kordofan, Sudan

Mohammed Abdelmanan^{1*}, Zhang Xiaoli, MulikAbbaker¹, Abdelrahim Omer, Nasereldin Adam, Salim Haroun

Forest Department, Faculty of Forestry Sciences, University of Zalingei, P.O.Box 06, Darfur, Sudan

Range Department, Faculty of Forestry Sciences, University of Zalingei, P.O.Box 06, Darfur,

Abstract: The North Kordofan State has undergone rapid, wide-ranging changes in land cover intensified by human activities and over grazing. This study examined the use of remote sensing data and geographic information system (GIS) techniques to gain a quantitative understanding of the spatiotemporal dynamics of land cover. In addition, the major factors behind land cover changes and expansion of Sand area were analyzed. A post-classification comparison approach was used to detect land cover changes in the study area between 2000 and 2020 using Landsat two images from 2000, and 2020. The observed changes were indicative of a decrease in the expanse of Acacia senegal Trees which gain (378.5814 km²) of its total area over 20 years. Results indicate an unstable trend of Sand area which generally increased. From the outcomes of this study, it is strongly recommended that urgent measures should be taken to conserve the vegetation cover. Moreover, this map documents constant reality in discrete land cover types which can be used by researchers and decision makers as the guide for future planning and development.

Keywords: Change detection; Maximum Likelihood Classification; Post-classification comparison; deforestation.

Date of Submission: 05-02-2022

Date of acceptance: 18-02-2022

I. INTRODUCTION

Change in land cover has been recognized as the global issue connected with land degradation and desertification (Bartholomé and Belward 2005; Sano et al. 2010; Shalaby and Tateishi 2007). Over the past decades, desert encroachment has drastically transformed North Kordofan land cover and influencing the ecosystem function. The south border of the desert has been moved to south with an average of 90-100 km through the last 17 years (El Gamri et al. 2009; Elhag 2006). This is affecting the land cover and expanding the desert area. However, desert encroachment damaged almost all the vegetation cover except trees and small patches of dunes adapted shrubs. The desert encroachment is seriously threat agricultural land and declining food production. According to (Ayoub 1998; Dawelbait and Morari 2012) the desert is continued moving to the south at a rate of 5-6 km per year. Consequently, the desertification is spreading like cancer elsewhere in North Kordofan State. Most importantly, the vegetation cover has decreased dramatically, as indicated by (Yagoub et al. 2017), but up to date detailed land cover map for North Kordofan and its spatial distribution still unknown. Thus, mapping the major land cover types in North Kordofan is needed for the decision-making process in order to manage the land resources in a sustainable manner. However, remote sensing data is an indispensable source for land cover monitoring (Foody 2001; Hansen and Loveland 2012; Rawat and Kumar 2015; Rogan et al. 2003; Schulz et al. 2010), and they are useful for land cover mapping (Chen et al. 2015; Gong et al. 2013; Mayaux et al. 2004). It was, therefore, used efficiently in different land cover classification, mapping and change detection studies using various satellite images with different resolutions (Baker et al. 2006; Friedl et al. 2002; Hansen et al. 2000; Hansen et al. 2013). This success of remote sensing satellites is attributed to a range of advantages such as a wide range of geographical coverage and multi-spectral bands in each single image. Moreover, the premise of using remote sensing data is basically based on the availability and accessibility of freely Landsat archived data since 2008, which offers a unique opportunity for mapping the major land cover types in the study area. Therefore, integration of remote sensing and geographic information system (GIS) techniques made possible to classify and map different land cover types. Land cover is very significant and easily detectable indicator for

measuring environmental change (Seppelt et al. 2011). In other words, it is a dynamic factor that is associated to the interaction between human activities and environmental changes. Therefore, there is an urgent need for mapping North Kordofan land cover for a wide range of purposes including decision-making process to sustainable land resources management. Moreover, North Kordofan is the one of the most important producing area of *Gum Arabic* at local, regional and international scales. In this study, our main objective is to map the major land cover types in using Landsat ETM+ images and to examine their spatial distribution in North Kordofan State. We would precisely want to answer the following scientific question:

- How accurately can Landsat ETM+ images produce a thematic map for land cover types in North Kordofan State?

II. MATERIALS AND METHODS

2.1. Study Area

North Kordofan state, located in semi-arid zone of Sudan, approximately from latitudes $12^{\circ} 40' N$ to $14^{\circ} 20' N$ and longitudes $28^{\circ} 10' E$ to $31^{\circ} 40' E$ (Fig. 1). North Kordofan covers an area of approximately $185,302 \text{ km}^2$. The state is unique in its natural resources. It is rich in agricultural products and rangeland resources which allow the raising of various kinds of livestock (sheep, camels, and cows). Animal husbandry is the backbone of the economy of the state and plays a major source of income for the majority of the inhabitants. Also, it's considered as one of the main areas of *Gum Arabic* producing at local, regional and international scales. The predominant climate is semi-arid, with dry cool in winter (December – January) and rainy season (July- October) with average annual rainfall ranging from 300–400 mm and a persistent feature of the climate in North Kordofan is drought.

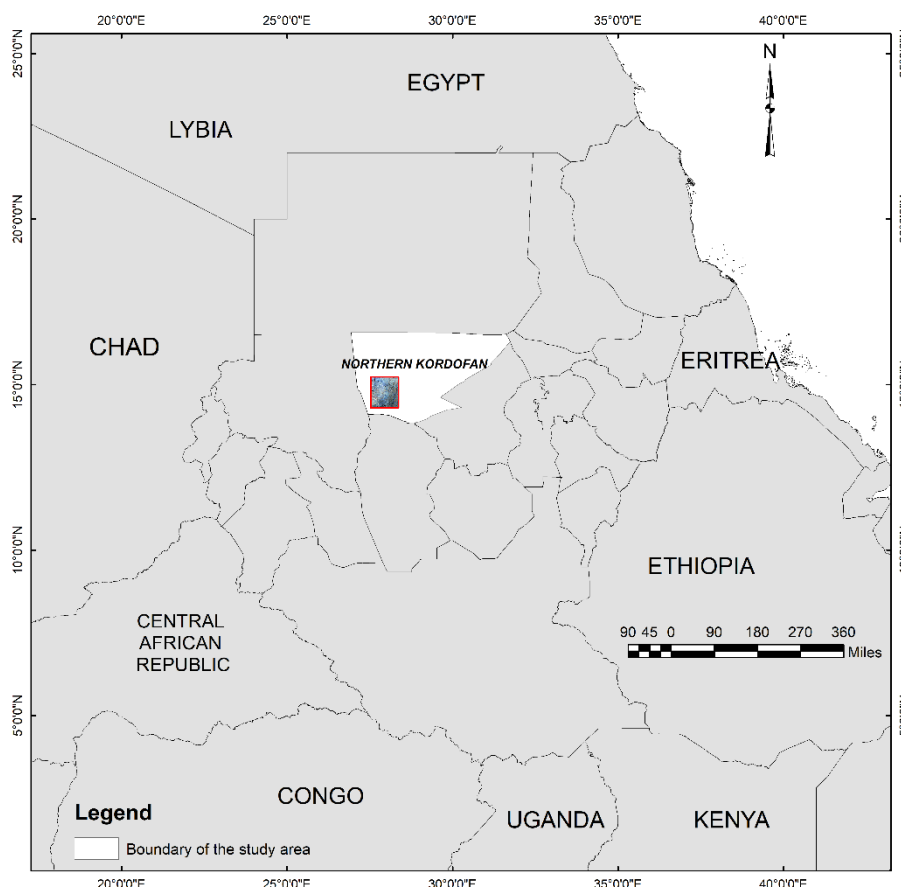


Figure 1. Location of region of interest in North Kordofan, Sudan

2.2. Data

Landsat ETM+ images located by satellite path/row 176/050 were used. The images were acquired free of cost from the archive database at <http://glovis.usgs.gov/> with the 0% of cloud cover. An extensive ground-points survey was carried out in the dry season from January to March 2015, a total of 105 ground-points as the reference data in North Kordofan and land cover characteristics were collected. The ground-points were

collected using handheld GPS device (GARMIN GPSMAP 60CSx), and used for accuracy assessment of the classification. Table 1 shows the characteristics of Landsat data used in this study.

Table 1.Source and characteristics of satellite imagery used in this study.

Datasets	Date	Spatial resolution scale, m	Spectral bands	Swath, km	Source	Format
Landsat 7 ETM+L1T	Nov. 2000	30	8 bands	185	http://glovis.usgs.gov/	GeoTiff
Landsat 7 ETM+L1T	Dec. 2020	30	8 bands	185	http://glovis.usgs.gov/	GeoTiff

2.3. Pre-processing

Geometric rectification is the most significant for producing spatially corrected map of land cover. Landsat TM image of 2010 was used as a reference to register Landsat ETM+ image. Image to image registration with the first-degree polynomial equation was performed. The nearest neighbor resampling technique was used to avoid changing the original pixel values of the image. Landsat ETM+ image of 2015 was geometrically corrected using 21 control points. The result of Root Mean Square (RMS) error was less than 0.7 pixels. Moreover, one of the more significant preconditions for remote sensing data analysis is the atmospheric correction which had been done by applying the Model FLAASH (Fast Line-of-Sight Atmospheric Analysis of spectral Hypercubes), in order to improve the image information by transforming the radiance as sensor into surface reflectance values. Then a new subset image contains the region of interest was created in each ETM+ images using the area of interest (AOI) function in ENVI 5.1 and the clip function in ArcMap 10.2. However, this is helpful and effective to reduce the image file size and thus we can focus just on the region of interest. The color composite of the image was generated from Landsat ETM+ bands 6, 5, and 3 as showed in Figure 2a. This color composite was chosen to assist the collection of the training and test data of each land cover class. Besides to the raw image input, normalized difference vegetation index (NDVI) as a simple statistical indicator that can be utilized to investigate the remote sensing measurements and assess whether the object being observed contains live green vegetation or not. However, we derived NDVI from the Landsat ETM+ images using the following equation (1).

$$NDVI = \frac{NIR-RED}{NIR+RED} \dots\dots\dots (1)$$

Where NIR and RED correspond to near-infrared and red spectral bands of Landsat ETM+ image

2.4. Image classification

Image classification was carried out using supervised classification technique based on Maximum Likelihood Classifier (MLC). After classification has been chosen, training test samples were carefully selected in sufficient homogeneity in order to symbolize spectral and spatial characteristics of each land cover types as well as maximize classification accuracy. This step is probably the most significant element of supervised classification, because the spectral signatures extracted from the training test samples will determine the overall accuracy of the classification and thus the utility of the final land cover map. Therefore homogeneity should be taken in choosing training test samples that represent different land cover types and avoiding heterogeneous areas. In this study, a modified version of the Anderson land use land cover classification system was used (Anderson 1976). While this classification system was basically developed for the USA, however, it is widely used worldwide (Alsaideh et al. 2012). The system established that land use/land cover classification of level 1 class can be mapped over large areas from Landsat data or high altitude imagery. Thus land use/land cover classification system of Level 1 was chosen and referred to the classification system of this study. Land cover classification scheme and detailed descriptions were illustrated in Table 2. A kernel size 3 x 3 was used to image smoothen and reduce the number of misclassified pixels. Also, the visual interpretation was carried out because it allows an integrated use of spectral and spatial contents as well as prior knowledge of the study area.

Table 2.Definition of land cover classes of classification scheme adopted in this study

Land cover	Description
Water Body	Area with seasonal water coverage, it the main source of drinking, cooking and other uses.
Natural Forest	The area covered by natural trees that covers almost 10% and considered as the main source of fodder for livestock and fuel wood.
Barren and Low Vegetation	Areas with low or no vegetation including rocky areas, areas of severe erosion that resulting from overgrazing or poor cultivation practices.

Acacia senegal Trees	Areas covered by a natural woody vegetation known as Acacia senegal Trees which characterized the area with cover reaching 15-17%, generally composed of trees less than 6m.
Sand	The areas that characterized by ongoing or recent sand encroachment.

2.5. Maximum Likelihood Classifier (MLC)

A maximum likelihood classifier (MLC) is one of the well- recognized parametric classifiers applied for supervised classification. According to (Guide 1999; Scharf 1991) the algorithm for computing the weighted distance or likelihood D of unknown measurement vector X belong to one of the known classes M_c is based on the Bayesian equation (2).

$$D = \ln(a_c) - [0.5\ln(|cov_c|)] - [0.5(X - M_c)T(cov_c - 1)(X - M_c)] \dots\dots\dots (2)$$

The unknown measurement vector is assigned to the class in which it has the highest probability of belonging. The advantage of the MLC as a parametric classifier is that takes into account the variance-covariance within the class of the normally distributed training data.

2.6. Accuracy assessment

Accuracy is usually used to determine the quality of the information generated from remote sensing data and the level of classification correctness. The accuracy was assessed by using 105 ground control points (GCPs) collected during the field survey in the study area. An error matrix as cross-tabulations of the mapped class vs. class reference was used to assess classification accuracy. Overall accuracy, user’s and producer’s accuracies were then calculated. Moreover, Kappa statistic was also derived for estimating the degree of classification accuracy as it not only account for diagonal elements but for whole confusion matrix elements.

III. RESULTS AND DISCUSSIONS

3.1 Accuracy assessment

The use of Maximum Likelihood Classifier (MLC) to classify the Landsat ETM+ images has produced maps showing the distribution of the five prevalent land cover classes in the region of interest for the years 2000, and 2020. Accuracy assessment was carried out for the classified maps of 2000 and 2020 to examine the agreement between the produced maps and what actually exists on the ground. Table 3 illustrates the summarized results of classification accuracy.

Table 3. Accuracy assessment for the classified maps of 2000 and 2020

Land cover	2000		2020	
	User’s	Producer’s	User’s	Producer’s
Water Body	64.3	75.0	78.6	91.6
Natural Forest	81.5	81.5	85.2	79.3
Barren and Low Vegetation	85.7	85.7	73.7	66.6
Acacia senegal Trees	93.7	88.2	80.0	80.0
Sand	82.4	87.5	82.9	87.1
Overall accuracy	85.7		80.4	
Kappa statistic	0.801		0.756	

The classified maps of 2000 and 2020 achieved overall accuracy values of 85.7% and 80.4%, respectively, indicating that both land cover maps met the criterion. Furthermore, values of the kappa statistic for both the two maps were more than 0.75, indicating good agreements.

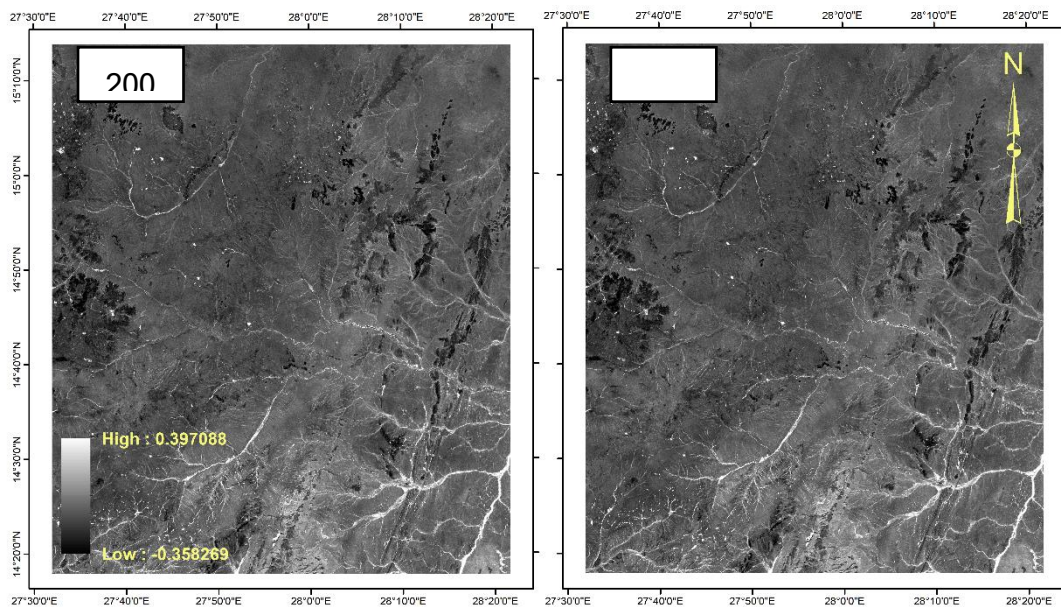


Figure 2: Grayscale maps showing a variance of NDVI for 2000 and 2020, which is most useful for separating vegetation cover from other land cover classes, the vegetation cover have much larger variance than sand.

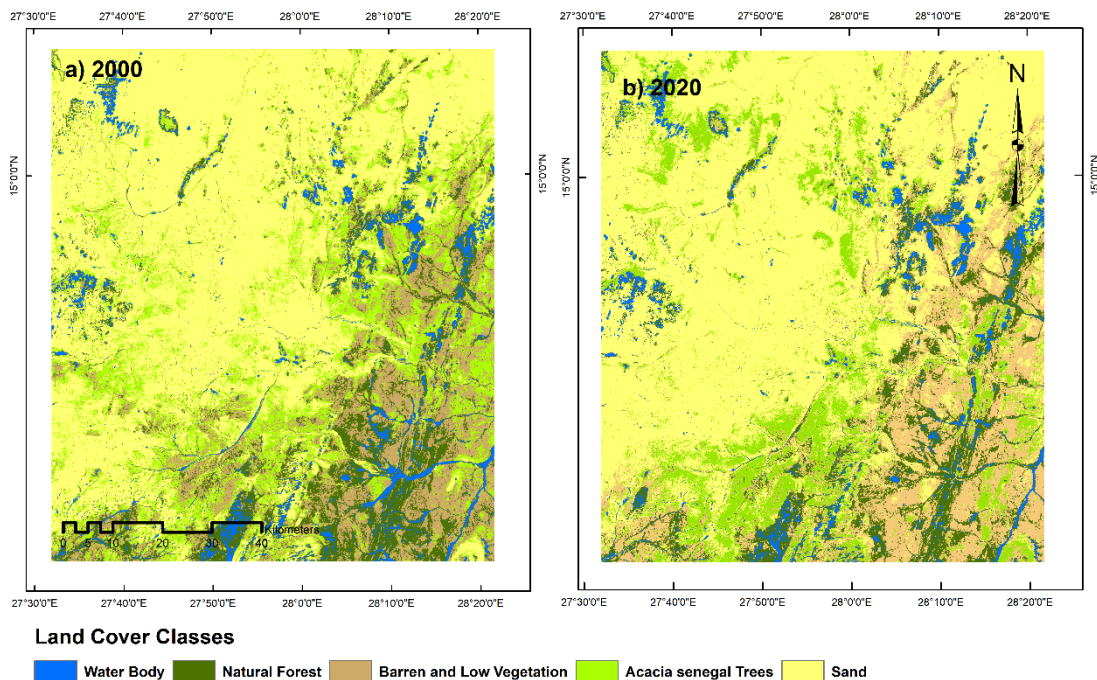


Figure 3. Classified maps of the region of interest based on supervised classification of 2000 and 2020 Landsat ETM+ images.

3.2 Supervised classification

The processing and supervised classification of Landsat ETM+ images acquired in 2000 and 2020 produced two classification maps for the five land cover types prevalent in the area of the interest (Figure 3). Classification results showed that the areas of land cover classes in the two produced maps (2000 and 2020) are in descending order as follows: Water Body, Natural Forest, Barren and Low Vegetation, *Acacia senegal* Trees, and Sand. Sand is the dominating class, especially in the northern latitudes of the study area, covering more than half of the total landscape in 2000 and 2020 but increased to more than 50% in 2020. The continuous sand encroachment takes place through a systematic movement of the desert southern boundary into south part of the study area which caused serious threat to the vegetation cover. Sand encroaches upon vegetative areas, mostly

after heavy sand storms, which are most frequent during the winter season. However, loss of productive lands was the major impact of sand encroachment on the environment along the study area. This negative impact would further lead to environmental changes in the future. The *Acacia senegal* Trees and Barren Low Vegetation classes occupied an area ranging from 17.95% to about 13.84% and 17.19% and 17.89%, in 2000 and 2020, respectively (Table 4). While the maximum area of each of the other classes represents less than 14% of the total area over the study time period. However, *Acacia senegal* Trees are the most significant types of vegetation, this species comprises of a pure stand over a large area which is mainly devoted to Gum Arabic production and livestock grazing. Notably, Water Body covers only 3.81% and 3.57% in 2000 and 2020, respectively. Water resource challenges have long existed in study area, but their impact amplified by recent trends such as rapid environmental change, economic growth and of course climate change.

3.3 Land cover change detection

The outcomes of the post-classification comparison give an account of the amount and type of change that has taken place for each land cover class. Areal change of land cover types over the study time period was obviously visible and occurred as either an expansion or a decline between sequential dates. Attempts to further study these outcomes can give insight to the land use behavior, pattern, and rate at which the changes occur in the study area in particular and in the North Kordofan State in general. This essential information would be vital for development planners and decision makers.

Change statistics for the periods of 2000-2020, were generated from the comparison of classified maps of 2000 and 2020 and will be discussed in the following sections.

Land cover change between 2000 and 2020

In 2000, the Sand class constituted the largest type of land cover class in the study area at 51.09% of the total area, followed by *Acacia senegal* Trees (17.95%), Barren Low Vegetation (17.9%), and Natural Forest (9.96%), whereas Water Body only covered 3.81% and occupied the smallest area. During the 20-year time frame from 2000 to 2020, the area covered by Sand and Barren Low Vegetation were expanded by 341.496 and 64.0548, respectively, while other land cover classes decreased at different rates. Table 4 and Figure 4 summarize the change occurred within the study area between 2000 and 2020.

Table 4. Area coverage of land cover types in km² and changed area from 2000 to 2020.

No	Land cover	Area in km ²		Area in %		Changed Area in Km ² from 2000 to 2020
		2000	2020	2000	2020	
1	Water Body	351.1647	328.7295	3.81	3.57	-22.4352
2	Natural Forest	917.9505	913.4163	9.96	9.91	-4.5342
3	Barren and Low Vegetation	1584.8055	1648.8603	17.19	17.89	64.0548
4	<i>Acacia senegal</i> Trees	1654.1415	1275.5601	17.95	13.84	-378.5814
5	Sand	4709.1456	5050.6416	51.09	54.80	341.496
	Total	9217.2078	9217.2078	100	100	

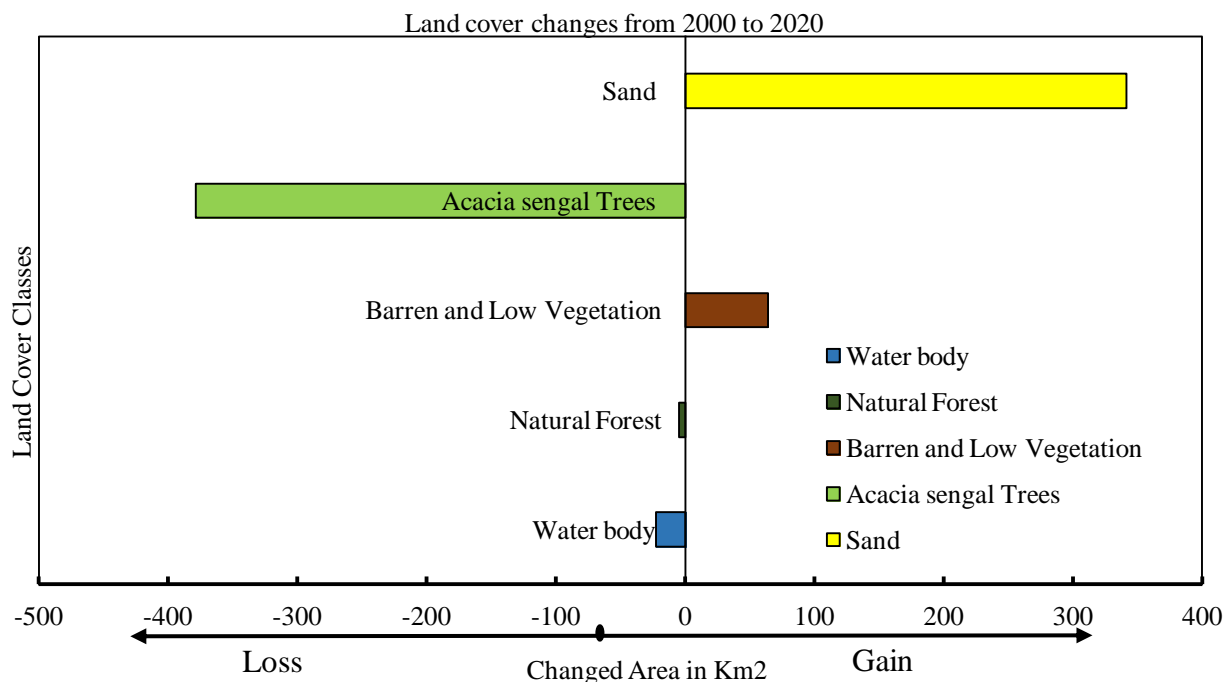


Figure 4. Net loss and gain for each land cover class for the period 2000-2020

As shown in Table 4, based on 9217.2078km², the total size of the study area, Sand covered 4709.1456 km² in 2000 (51.09% of the total area), but this changed to 5050.6416 km² (54.80%) in the year 2020, with a positive rate of change of 341.496 km². As shown in Figure 4, out of 1654.1415 km² that was *Acacia senegal* Trees in 2000, about (378.5814 km²) loss) in 2020. The changed area was either cleared or converted to other land cover classes, mostly for grazing purposes. The lack of awareness among other factors encouraged the local people to engage in cutting *Acacia senegal* Trees for firewood and producing charcoal. Destructive of *Acacia senegal* Trees have always been present since the past few decades and its negative effects were visible and tangible.

The results shown in Table 4 indicate that the Natural Forest areas, which amounted to (917.9505 km²) in 2000, decreased to (913.4163 km²) in 2020. The decrease in Natural Forest might be attributed to consequent livestock browsing and increase in firewood demand. On the other hand the period 2000-2020 experienced severe droughts. Cutting Natural Forest is a negative phenomenon that can lead to stripping plenty of spaces of their natural vegetation cover. In fact, in such a semi-arid climate, the loss of natural trees is difficult to recover due to the inability of the existing tree species to regenerate naturally in addition to other limiting factors such as insufficient moisture due to frequent droughts and soil shallowness resulting from increased erosion rate after removal of trees.

IV. CONCLUSION

At local scale, remote sensing can accurately map the natural resources. The results of this study show the importance of satellite image processing with the aid of GIS techniques in mapping and detecting land cover changes. Supervised classification of Landsat ETM+ with Maximum Likelihood and post-classification comparison approach can be used to predict and obtain fairly accurate maps of land cover changes. The overall accuracy and kappa statistics values of the land cover classifications achieved in this study are encouraging. It was generally observed that there was a significant decline in *Acacia senegal* Trees and a corresponding increase in Sand. The changes observed were indicative of an increase in the expanse of Sand area, which gained about (341.496 km²) of its total area over the 20 years, and the slight deforestation rate was registered in the period (2000–2020). The slight deforestation was generally a result of local people engaging in cutting *Acacia senegal* Trees for firewood and producing charcoal. Land under the Barren and Low Vegetation class increased by about (64.0548 km²) and achieved a greater rate of increase from 2000 to 2020, whereas the land under the Water Body class decreased by about (22.4352) between 2000 and 2020. Our results indicate an unstable trend of Sand area which generally increased significantly during the period between 2000 and 2020.

Indeed, if the present trend of Sand are continues, the Sand in the study area will gain more than 50% of its current sand class over the next 10 years. Sand encouragement in the study area and North Kordofan State in general is an important environmental challenge.

ACKNOWLEDGEMENTS

The authors would like gratefully acknowledge the financial support of the China Scholarships Council (CSC). We are also grateful to the United State Geographical Survey (USGS) for providing remote sensing data. We also thank all the colleagues and those who contributed in any way to achieve the goal of the study.

Conflicts of Interest: The authors declare no conflict of interest.

REFERENCES

- [1]. Alsaadeh, B., Al-Hanbali, A., & Tateishi, R. (2012). Assessment of land use/cover change and urban expansion of the central part of Jordan using remote sensing and GIS. *Asian Journal of Geoinformatics*, 11
- [2]. Anderson, J.R. (1976). *A land use and land cover classification system for use with remote sensor data*. US Government Printing Office
- [3]. Ayoub, A.T. (1998). Extent, severity and causative factors of land degradation in the Sudan. *Journal of Arid Environments*, 38, 397-409
- [4]. Baker, C., Lawrence, R., Montagne, C., & Patten, D. (2006). Mapping wetlands and riparian areas using Landsat ETM+ imagery and decision-tree-based models. *Wetlands*, 26, 465-474
- [5]. Bartholomé, E., & Belward, A. (2005). GLC2000: a new approach to global land cover mapping from Earth observation data. *International Journal of Remote Sensing*, 26, 1959-1977
- [6]. Chen, J., Chen, J., Liao, A., Cao, X., Chen, L., Chen, X., He, C., Han, G., Peng, S., & Lu, M. (2015). Global land cover mapping at 30m resolution: A POK-based operational approach. *ISPRS Journal of Photogrammetry and Remote Sensing*, 103, 7-27
- [7]. Dawelbait, M., & Morari, F. (2012). Monitoring desertification in a Savannah region in Sudan using Landsat images and spectral mixture analysis. *Journal of Arid Environments*, 80, 45-55
- [8]. El Gamri, T., Saeed, A.B., & Abdalla, A. (2009). Rainfall of the Sudan: characteristics and prediction. *Arts J*, 27, 18-35
- [9]. Elhag, M.M. (2006). Causes and impact of desertification in the Butana area of Sudan. In: University of the Free State
- [10]. Foody, G. (2001). Monitoring the magnitude of land-cover change around the southern limits of the Sahara. *Photogrammetric Engineering and Remote Sensing*, 67, 841-848
- [11]. Friedl, M.A., McIver, D.K., Hodges, J.C., Zhang, X., Muchoney, D., Strahler, A.H., Woodcock, C.E., Gopal, S., Schneider, A., & Cooper, A. (2002). Global land cover mapping from MODIS: algorithms and early results. *Remote sensing of Environment*, 83, 287-302
- [12]. Gong, P., Wang, J., Yu, L., Zhao, Y., Zhao, Y., Liang, L., Niu, Z., Huang, X., Fu, H., & Liu, S. (2013). Finer resolution observation and monitoring of global land cover: First mapping results with Landsat TM and ETM+ data. *International journal of remote sensing*, 34, 2607-2654
- [13]. Guide, E.F. (1999). *Erdas. Inc. Atlanta, Georgia*, 18
- [14]. Hansen, M., DeFries, R., Townshend, J.R., & Sohlberg, R. (2000). Global land cover classification at 1 km spatial resolution using a classification tree approach. *International Journal of Remote Sensing*, 21, 1331-1364
- [15]. Hansen, M.C., & Loveland, T.R. (2012). A review of large area monitoring of land cover change using Landsat data. *Remote Sensing of Environment*, 122, 66-74
- [16]. Hansen, M.C., Potapov, P.V., Moore, R., Hancher, M., Turubanova, S., Tyukavina, A., Thau, D., Stehman, S., Goetz, S., & Loveland, T. (2013). High-resolution global maps of 21st-century forest cover change. *science*, 342, 850-853
- [17]. Mayaux, P., Bartholomé, E., Fritz, S., & Belward, A. (2004). A new land-cover map of Africa for the year 2000. *Journal of Biogeography*, 31, 861-877
- [18]. Rawat, J., & Kumar, M. (2015). Monitoring land use/cover change using remote sensing and GIS techniques: A case study of Hawalbagh block, district Almora, Uttarakhand, India. *The Egyptian Journal of Remote Sensing and Space Science*, 18, 77-84
- [19]. Rogan, J., Miller, J., Stow, D., Franklin, J., Levien, L., & Fischer, C. (2003). Land-cover change monitoring with classification trees using Landsat TM and ancillary data. *Photogrammetric Engineering & Remote Sensing*, 69, 793-804
- [20]. Sano, E.E., Rosa, R., Brito, J.L., & Ferreira, L.G. (2010). Land cover mapping of the tropical savanna region in Brazil. *Environmental Monitoring and Assessment*, 166, 113-124
- [21]. Scharf, L.L. (1991). *Statistical signal processing*. Addison-Wesley Reading, MA
- [22]. Schulz, J.J., Cayuela, L., Echeverria, C., Salas, J., & Benayas, J.M.R. (2010). Monitoring land cover change of the dryland forest landscape of Central Chile (1975–2008). *Applied Geography*, 30, 436-447
- [23]. Seppelt, R., Dormann, C.F., Eppink, F.V., Lautenbach, S., & Schmidt, S. (2011). A quantitative review of ecosystem service studies: approaches, shortcomings and the road ahead. *Journal of applied Ecology*, 48, 630-636
- [24]. Shalaby, A., & Tateishi, R.J.A.G. (2007). Remote sensing and GIS for mapping and monitoring land cover and land-use changes in the Northwestern coastal zone of Egypt, 27, 28-41
- [25]. Yagoub, Y.E., Li, Z., Musa, O.S., Anjum, M.N., Wang, F., Xu, C., & Bo, Z. (2017). Investigation of Vegetation Cover Change in Sudan by Using Modis Data. *Journal of Geographic Information System*, 9, 279

Mohammed Abdelmanan, et. al. "Monitoring of Rapid Land-cover Change in the Intensified Grazing Area of North Kordofan, Sudan." *American Journal of Engineering Research (AJER)*, vol. 11(02), 2022, pp. 26-33.